# Temperature Dependence of the Liquid-Vapor Isotopic Fractionation Factors in $CD_3H$-$CH_4$ and $CD_3F$-$CH_3F$ Mixtures*

Anthony M. Popowicz[a], Ting-Hai Lu[b] and Jacob Bigeleisen[c]

Department of Chemistry, State University of New York, Stony Brook, Stony Brook, New York 11794-3400

Z. Naturforsch. **46a**, 60–68 (1991); received August 8, 1990

*Unserem Kollegen, Herrn Dr. Karl Heinzinger, zum 60. Geburtstag gewidmet*

The liquid-vapor isotope fractionation factors, LVIFF, $\alpha = CD_3X/CH_3X)_l/(CD_3X/CH_3X)_v$, of $CD_3H$–$CH_4$ and $CD_3F$–$CH_3F$ mixtures have been measured from 102–160 K and 182–254 K, respectively. The results are in good agreement with previous vapor pressure ratios, VPIE, which cover the ranges 90–112 K and 132–211 K, respectively. Over the temperature ranges of the LVIFF measurements, $\ln \alpha$ is negative for the $CD_3H$–$CH_4$ mixture and positive for the $CD_3F$–$CH_3F$ mixture. There is significant curvature in a plot of $T^2 \ln \alpha$ vs. $T$ for the $CD_3H$–$CH_4$ mixture. The curvature is related to the densities of the liquid and vapor phases. It is shown that an expansion of the pair correlation function up to powers of the square of the densities of the liquid and vapor phases accounts for the $T^2 \ln \alpha$ vs. $T$ curvature and leads to $\ln \alpha$ equal to zero at the critical temperature. Correction of the LVIFF values of $T^2 \ln \alpha$ for the density effect gives values for the contributions of translation, rotation and internal vibration in good agreement with previous cell model calculations. Similar treatment of the LVIFF data on the $CD_3F$–$CH_3F$ mixture leads to the conclusion that the internal zero point energy effect on the differences in the heats of vaporization of $CH_3F$ and $CD_3F$ makes a small contribution to the overall difference in free energies of vaporization.

## Introduction

All the pre-1960 data on vapor pressure isotope effects (VPIE) and liquid-vapor isotope fractionation factors (LVIFF) for molecular fluids and solids can be represented by empirical equations of the form [1]

$$\ln \alpha = \ln (P'/P) \{1 + P (B_0 - V_c/RT)\} = \frac{A}{T^2} - \frac{B}{T}. \quad (1)$$

The prime refers to the light molecule and $\alpha$ is defined in the Abstract. The empirical constants $A$ and $B$ have been related to the molecular properties of the condensed and vapor phases. In the approximation that the molecular vibrations are harmonic oscillators one obtains through the application of statistical mechanics to the equilibrium between a condensed phase and its vapor [2–5].

$$A = (1/24)(h/kT)^2 \left( \left( \frac{1}{M'} - \frac{1}{M} \right) (\langle \nabla^2 U \rangle_c - \langle \nabla^2 U \rangle_v) + \left( \frac{1}{I'} - \frac{1}{I} \right) (\langle O^2 U \rangle_c - \langle O^2 U \rangle_v) + \ldots \right), \quad (2)$$

$$B = (hc/2k) \sum_i (\nu'_{iv} - \nu'_{ic}) - (\nu_{iv} - \nu_{ic}). \quad (3)$$

The terms in (1)–(3) have been previously defined [1]. The $A$ term gives the contribution to the logarithm of the vapor pressure ratio or the logarithm of the isotope separation factor, $\alpha$, from the difference in the Laplacian of the intermolecular potential in the condensed and vapor phases. It includes contributions from translation, $(1/M' - 1/M)$, rotation, $(1/I' - 1/I)$, and correction terms from the coupling of translation and rotation in the condensed phase. The $B$ term gives the contribution from the shift in the internal vibrations from the gas to the condensed phase in the zero point energy approximation. The exact statistical mechanical expression for the above model includes an entropy term, $\sum_i \ln (u_i/u'_i)_c/(u_i/u'_i)_v$, and the Boltz-

* Research supported in part by the Division of Basic Energy Sciences, US Department of Energy, Contract DEAC02-79ER10346.

[a] Present address – Rockefeller University, Smith Hall-B5, 1230 York Ave., New York, N.Y. 10021-6399.

[b] Present address – Institute of Atomic Energy, P.O. Box 275 (22), Beijing, People's Republic of China.

[c] To whom correspondence about this article should be addressed.

Reprint requests to Prof. J. Bigeleisen, Department of Chemistry, State University of New York, Stony Brook, New York 11794-3400, U.S.A.

mann excitation terms, $\sum_i \ln[(1-e^{-u_i'})/(1-e^{-u_i})]_c - \ln[(1-e^{-u_i'})/(1-e^{-u_i})]_v$. These correction terms are discussed in Appendix I.

In the harmonic oscillator approximation for the molecular motion in the condensed phase, and when the vapor is dilute, $A$ reduces to

$$A=(1/24)(h\,c/k)^2 \sum_i^6 (\nu_i'^2-\nu_i^2)_{ext}. \quad (4)$$

The $A$–$B$ equation (1) has been shown to be very useful in the correlation and understanding of condensed phase isotope effects [1]. It properly predicts the crossover phenomenon, the inverse isotope effects found with deuterocarbons ($B > A/T$), the role of hindered rotation and numerous types of coupling in the condensed phase which have been observed through condensed phase isotope effect studies. These include translation-rotation coupling, rotation-internal vibration coupling and translation-internal vibration coupling.

The definitive measurements of Bigeleisen and Roth [6] on the vapor pressure isotope effects in solid and liquid neon clearly established that anharmonic effects must be included to account for the temperature dependence of the isotope effect in the solid. Anharmonic effects in the solid, the large coefficient of expansion of liquids as well as the fact that the isotope separation factor must equal unity at the critical temperature provided an impetus to broaden the temperature range of VPIE and LVIFF studies and improve the precision of condensed phase isotope effect measurements. This program was initiated in 1964 and led to a new generation of cryostats for such studies [4, 7, 8].

Van Hook [9] showed, in his study of the vapor pressure isotope effects of the complete series of liquid deuteroethanes, that plots of $\ln(P/P')$ vs. $1/T$ have maxima as predicted by (1). The position of the maximum depends on the extent of deuteration and differs between equivalent isomers. The slopes of $\ln(P/P')$ vs. $1/T$ on the two sides of the maximum for any isomer are not equal. Therefore, the temperature dependence of the VPIE of the deuteroethanes cannot be explained by (1). Van Hook introduced temperature dependent force constants for the external modes and the hindered rotation, which accounted for the asymmetry with respect to the maxima in the $\ln(P/P')$ vs. $1/T$ plots. Extensive studies on the deuteroethylenes [10, 11] showed that the earlier data of Bigeleisen, Ribnikar and Van Hook [12], which could be fit by (1), required temperature dependent $A$ and $B$ terms.

Experimental measurements of the VPIE and LVIFF in the condensed rare gases, particularly argon, which cover the range from the low temperature solid through the melting point and to within 0.4 K of the critical temperature [4], and theoretical studies [13] established the temperature dependence of $\langle V^2U\rangle_l - \langle V^2U\rangle_v$) for the rare gases. Along the coexistence line of the liquid, from the triple point to the critical temperature, one finds from experiment and with theoretical justification [13]

$$\langle V^2U^*\rangle = C\,\varrho^*(1+\varrho^*), \quad (5)$$

where $U^*$ and $\varrho^*$ are the intermolecular potential and the density in reduced units, $U^*=U/RT_c$ and $\varrho^*=\varrho/\varrho_c$. From (1) and (5) one predicts and finds $T^2\ln\alpha/(\varrho_l-\varrho_g)(\varrho_c+\varrho_l+\varrho_g)$ for monatomic fluids almost independent of temperature over the entire liquid range. One finds a scaling law for $\alpha$ such that [4, 14]

$$T^2\ln\alpha = f(M)(\langle V^2U\rangle_l - \langle V^2U\rangle_v) = a(1-T^*)^b. \quad (6)$$

The scaling law for $\alpha$ is related to the scaling law for the liquid density,

$$(\varrho_l-\varrho_v)\approx(1-T^*)^\beta \quad (7)$$

by the relation [13, 14]

$$b-\beta=(1-T^*)/(3-T^*). \quad (8)$$

Götz, Lee and Bigeleisen [15] have measured the $^{13}C$ and $^{18}O$ LVIFF for CO over a wide temperature range. In this system hindered rotation and coupling of both the kinetic and potential energies of translation and rotation, in addition to the pure translation, contribute to the isotope effect. They analyzed their results by calculating the potential energy terms from spectroscopic data and vapor pressure isotope effects at 77.5 K. The temperature dependence of the translation can be calculated from (5). The sum of the squares of the librational modes of a number of simple linear molecules has been found empirically to be proportional to $\varrho^3$ in the solid. This temperature dependence was assumed for $\langle O^2U\rangle$. The calculations are in good agreement with the $^{18}O/^{16}O$ isotope fractionation data over the entire temperature range of the measurements. On the other hand, the calculated values of the $^{13}C/^{12}C$ fractionation factors have a larger temperature dependence than the experimental data. This suggests that $\langle O^2U\rangle$ has a slower dependence on the liquid density than $\varrho^3$.

The present experiments were undertaken to investigate the temperature dependence of the contributions of the internal vibrations to the vapor pressure isotope effect. The contribution of the internal vibrations, $B$ term in (1), are principally a zero point energy shift. Direct spectroscopic observations alone do not give the ground state zero point energy in a condensed phase because of the dielectric shift [16, 19]. Two systems were chosen for investigation, deuterium substitution in methane and methyl fluoride. In the case of methane there is the usual red shift of the C–H vibrations in the liquid phase compared with the vapor with the result that deuteromethanes have higher vapor pressures than the protium isomer at high temperatures and show the cross over at low temperatures [20]. In the case of methyl fluoride the D/H VPIE is normal [21]. The two largest contributions to the deuterium VPIE in methyl fluoride come from a blue shift in the asymmetric C–H stretching vibration and a red shift in the F–$CH_3$ stretching mode. These internal shifts essentially cancel one another with the result that the observed normal vapor pressure isotope effect has significant contributions from the symmetric C–H stretching mode, the $CH_2$ bending mode and the hindered rotation around the C–F axis.

The contributions from translation, rotation and internal vibration to the VPIEs in the liquid in equilibrium with vapor at low density have been analyzed in detail for these systems [21, 22]. These analyzes will facilitate the interpretation of the vapor pressure isotope effect of the liquid in equilibrium with high density vapors.

## Method

The reduced partition function ratio of a condensed phase, $(s/s')f_c$, relative to that of a real gas, $(s/s')f_r$, or an ideal gas, $(s/s')f_g$, can be evaluated either from VPIE or LVIFF data. The liquid-vapor isotope fractionation method, which can easily go to temperatures at which the vapor pressure is 50 atmospheres, was the method of choice in the present investigation. The reduced partition function ratio of the condensed phase relative to the real gas is related to $\alpha$ by the equation [4]

$$\ln (f_c/f_r)_{V_c, V_v} = \ln \alpha. \tag{9}$$

It is related to the isotopic vapor pressure ratio by

$$\ln (f_c/f_r)_{V_c, V_v} = \ln (P'/P)\{1 + P(B_0 - V_c/RT)\}. \tag{10}$$

In the literature, generally

$$\ln (P'/P)\{1 + P'(B'_0 - V_c/RT)\} \tag{11}$$

is tabulated, which is equal to $\ln (f_c/f_g)$ when there is no isotope effect on the equation of state of the real gas, $B'_0 = B_0$, and the molal volumes of the two pure isotopes in the condensed phase, $V'_c$ and $V_c$, are equal. In general the corrections from the latter assumption are negligible. The quantity (11) differs from (10) by the second order term $P(B'_0 - B_0)\{\ln (P'/P)\}^2$. Measurements of $\ln \alpha$ can be directly compared with the values tabulated as $\ln (f_c/f_g)$.

The cryostat and the gas handling systems have been described previously [4, 7, 23]. A major modification was made to the liquid sampling system. Previous measurements showed that flash evaporation from a capillary immersed in the liquid leads to isotopic fractionation and does not give a representative sample of the liquid. After testing a number of unsuccessful prototypes, a design for a valve assembly was developed which produced a piece of equipment which has the capability of isolating a representative sample of the liquid over a wide range of temperatures and pressures, and transferring it quantitatively out of the cryostat for isotopic analysis. A description of the valve design, construction and operation follows.

The valve assembly is shown schematically to scale in Figure 1. Release of the pressure acting on a pneumatically driven bellows valve, HPS, causes the valve to open. A sample of the liquid enters and fills a small previously evacuated chamber (vol. 0.043 ml). The valve is closed and then the sample is withdrawn by opening the LPS valve and transferring the sample from the sample chamber by vaporization. The entire valve assembly is connected to the flange which closes the top of the equilibration vessel. Apart from the valve tips, which are Kel-F, the valve is constructed of #304 stainless steel. The valve base is aligned and positioned with respect to the top of the flange by three threaded rods, which are not shown in the diagram. The maximum travel of the bellows to open or close either the HPS or LPS valves is 0.5 mm. Both helium and nitrogen gas were used to drive the bellows. With a pressure differential of 3 atmospheres across either valve seat at an absolute pressure of 1 atmosphere in the equilibration vessel, the leak rate across the seat of the valve was less than $4 \times 10^{-11}$ ml (NTP) helium/sec. The pressure necessary to seal the valve rose with the operating pressure and reached 40 atmospheres when the ambient pressure was

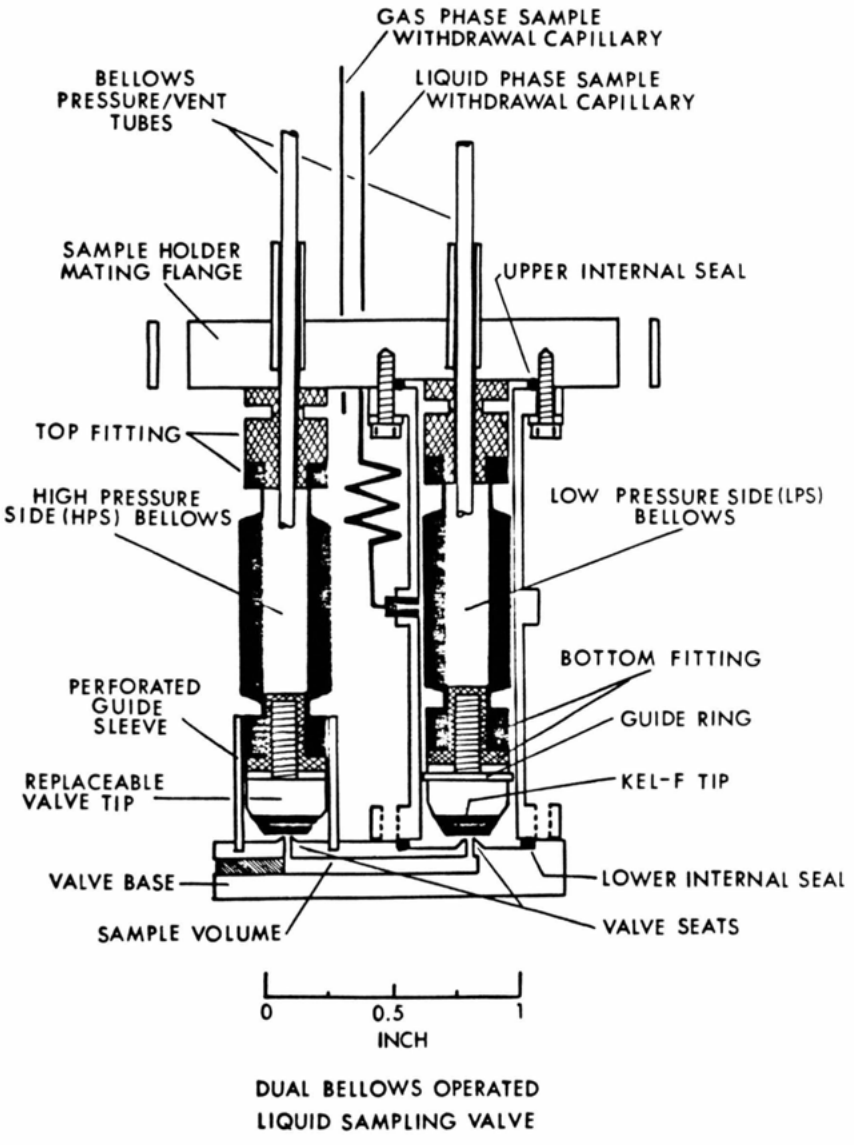


Fig. 1. Scale drawing of the non-fractionating liquid sampling valve.

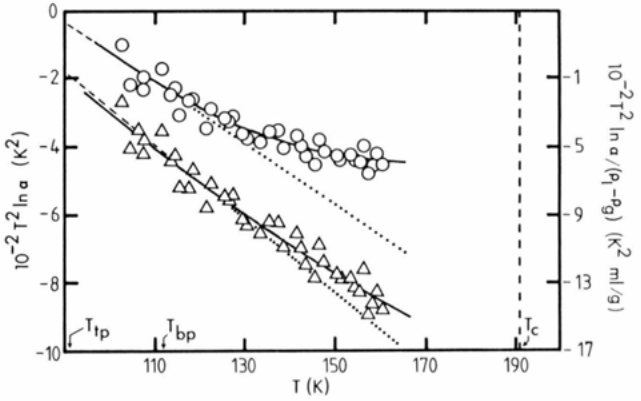


Fig. 2. Plots of $T^2 \ln \alpha$ —○—, and $T^2 \ln \alpha/(\varrho_l - \varrho_v)$ —△— vs. $T$, this work. $\alpha = (CD_3H/CH_4)_l/(CD_3H/CH_4)_v$. -----, linear least squares fit of the Armstrong, Brickwedde and Scott data [20]. ·····, extrapolation of the Armstrong, Brickwedde, and Scott data. $T_{tp} = 90.66$ K, $T_{bp} = 111.54$ K, $T_c = 190.6$ K.

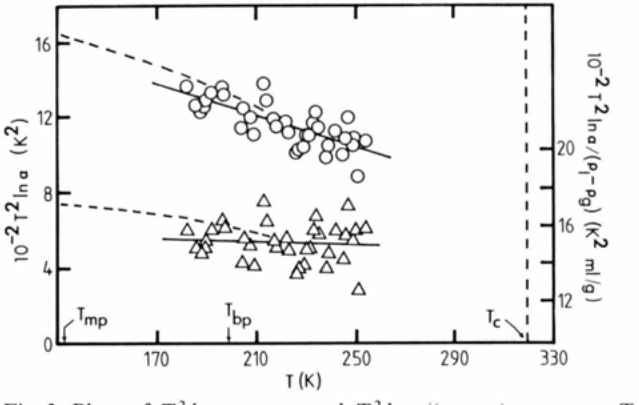


Fig. 3. Plots of $T^2 \ln \alpha$ —○—, and $T^2 \ln \alpha/(\varrho_l - \varrho_v)$ —△— vs. $T$, this work. $\alpha = (CD_3F/CH_3)_l/(CD_3H/CH_3F)_v$. -----, least squares fits of the Oi, Shulman, Popowicz, and Ishida data [21]. $T_{tp} = 131.35$ K, $T_{bp} = 194.80$ K, $T_c = 317.8$ K.

15 atmospheres. The valve performed completely reproducibly over hundreds of cycles in the temperature range 78–300 K.

The sampling procedure was tested for fractionation by the analysis of a sample of a liquid ethane-propane mixture. The liquid-vapor fractionation factor of a 40 mol percent ethane – 60 mol percent propane mixture at 205 K is 9.9. Two tests were made, one at 205.3 K and the other at 206.0 K. In the first test, the ethane/propane ratio of the bulk liquid was 0.542. Gas chromatographic analysis of a sample of the liquid withdrawn by the sampling valve gave 0.55 $\pm 0.02$. In the second test the analyzed value of 0.61 $\pm 0.02$ is to be compared with the known value 0.608. The sampling valve operated reliably and introduced no fractionation.

The fractionation factor is defined as

$$\alpha = (CD_3X/CH_3X)_l/(CD_3X/CH_3X)_v, \qquad (12)$$

where X = H or X = F. The ratios were determined by isotope ratio mass spectroscopy after quantitative conversion of the samples to dihydrogen gas. This avoids corrections for $^{13}C$ and the fragmentation of the parent molecule on electron bombardment. We define $R_l$ and $R_g$ as the corrected $(HD/H_2)$ ratios of the dihydrogen gas samples from the liquid and vapor phases, respectively. The (D/H) ratio in any sample is equal to the (D/H) ratio in the dihydrogen gas obtained by conversion. From stoichiometry one obtains

$$\ln \alpha (CD_3H/CH_4) = (1 + R_g/6)[\ln (R_l/R_g)] \qquad (13)$$

and

$$\ln \alpha (CD_3F/CH_3F) = [\ln (R_l/R_g)]. \qquad (14)$$

The samples of deuteromethane had values of $R_g$ near $1.4 \times 10^{-2}$ and thus corrections to the measured ratios, $R_l/R_g$, are small. Samples were converted to dihydrogen gas by passage over uranium turnings at 900 °C [24]. The reaction of carbon containing compounds with uranium metal coats the metal with uranium carbide. As a result the surface needs periodic regeneration. In our setup regeneration was carried out by treatment of the uranium with nitric acid after the conversion of about 25 samples of $1.6 \times 10^{-4}$ moles each.

The isotope ratio analyses were performed using standard procedures, which involves the correction of the mass 3 peak for $H_3^+$ and intercomparison of each sample with a standard [25]. In our setup the $H_3^+/H_2^+$ correction to the measured 3/2 ratio was typically of the order of 0.1% of the 3/2 ratio. By interfacing a signal averager, HP 3088 B, to a small microprocessor, HP 9866 A, to a Nuclide custom 6–60 isotope ratio mass spectrometer a precision of $\pm 0.02\%$ was obtained in the measurement of $R_l/R_g$. Approximately one mole each of $CD_3H$ in $CH_4$ and $CD_3F$ in $CH_3F$ mixtures were prepared by dilution of $CD_3H$ and $CD_3F$, respectively. The final mixtures each contained about 0.7 atom percent deuterium. The methane mixture, prepared from Matheson research grade methane (99.99% pure) and Merck, Sharpe and Dohme $CD_3H$ (98 atom% D) was found to be 99.95 pure by gas chromatography and was used without further purification. The methyl fluoride sample prepared from Linde (99%) methyl fluoride and Prochem $CD_3F$ (98 atom% D) was purified to 99.90% purity after removing $H_2O$, $CO_2$ and $CH_3Cl$ impurities by passage over soda-lime and then followed by a series of bulb to bulb distillations. The remaining impurities were 0.02% $CO_2$ and 0.08% $H_2O$, neither of which interfere in the liquid-vapor fractionating experiments.

Temperature were measured by means of a calibrated platinum resistance thermometer.

## Results

Measurements were made on the $CD_3H$–$CH_4$ mixture in the temperature range 102.7–160.6 K and on the $CD_3F$–$CH_3F$ mixture in the temperature range 182.0–254.3 K. The data are given in Table 1. Least squares fits to the data along with fits of the literature VPIE data are given in Table 2. The data are fitted to three functional equations:

$$T^2 \ln \alpha = A_1 - B_1 (T - T_0) + C_1 (T - T_0)^2, \qquad (15)$$

$$T^2 \ln \alpha/(\varrho_l - \varrho_v) = A_2 - B_2 (T - T_0) + C_2 (T - T_0)^2, \qquad (16)$$

and

$$T^2 \ln \alpha/(\varrho_l - \varrho_v)(\varrho_c + \varrho_l + \varrho_v) = A_3 - B_3 T. \qquad (17)$$

Plots of $T^2 \ln \alpha$ and $T^2 \ln \alpha/(\varrho_l - \varrho_v)$ for $CD_3H$–$CH_4$ and $CD_3F$–$CH_3F$ are given in Figs. 2 and 3, respectively. Neither the VPIE nor the LVIFF data on the methyl fluoride system show curvature in a plot of $T^2 \ln \alpha$ vs. $T$. Accordingly, the $C$ term in (15) and (16) is retained only for the present methane data. Over the temperature range 102–111 K, which is the common range for the VPIE and LVIFF $CD_3H$–$CH_4$ data, the

Table 1. Experimental values of $T^2 \ln \alpha$ for the liquid-vapor isotope fractionation factor in $CD_3H$–$CH_4$ and $CD_3F$–$CH_3F$ mixtures.

| $\alpha=(CD_3H/CH_4)_l/(CD_3H/CH_4)_v$ | | | $\alpha=(CD_3F/CH_3F)_l/(CD_3F/CH_3F)_v$ | | |
|---|---|---|---|---|---|
| $T$(K) | $T^2 \ln \alpha$ (K$^2$) | Run | $T$(K) | $T^2 \ln \alpha$ (K$^2$) | Run |
| 102.66 | − 98 | 1 | 182.02 | 1368 | 1 |
| 104.46 | −218 | 1 | 185.61 | 1267 | 1 |
| 106.35 | −168 | 2 | 187.68 | 1233 | 1 |
| 107.41 | −230 | 1 | 189.05 | 1256 | 3 |
| 107.42 | −193 | 2 | 189.62 | 1286 | 1 |
| 111.44 | −170 | 1 | 191.90 | 1332 | 1 |
| 113.41 | −246 | 1 | 196.24 | 1361 | 3 |
| 114.41 | −227 | 2 | 197.04 | 1321 | 2 |
| 115.41 | −306 | 1 | 204.10 | 1141 | 3 |
| 117.47 | −264 | 1 | 204.97 | 1248 | 2 |
| 118.38 | −258 | 2 | 207.28 | 1201 | 3 |
| 121.38 | −345 | 1 | 209.02 | 1107 | 2 |
| 122.38 | −288 | 2 | 213.08 | 1379 | 2 |
| 125.38 | −315 | 1 | 214.27 | 1289 | 3 |
| 126.37 | −321 | 2 | 217.04 | 1191 | 2 |
| 127.35 | −309 | 1 | 218.18 | 1152 | 3 |
| 129.40 | −361 | 1 | 222.10 | 1178 | 3 |
| 130.38 | −374 | 2 | 223.06 | 1120 | 1 |
| 133.35 | −386 | 1 | 226.15 | 1013 | 3 |
| 135.37 | −354 | 1 | 227.08 | 1033 | 1 |
| 137.37 | −352 | 1 | 229.08 | 1038 | 1 |
| 138.49 | −403 | 2 | 230.22 | 1101 | 3 |
| 141.47 | −367 | 1 | 231.13 | 1101 | 1 |
| 142.45 | −395 | 2 | 233.13 | 1171 | 1 |
| 143.49 | −428 | 1 | 234.15 | 1225 | 3 |
| 145.49 | −451 | 1 | 235.13 | 1147 | 2 |
| 146.46 | −378 | 2 | 238.17 | 991 | 3 |
| 147.51 | −410 | 1 | 239.12 | 1046 | 2 |
| 150.44 | −425 | 2 | 241.98 | 1125 | 3 |
| 151.33 | −433 | 1 | 244.97 | 998 | 2 |
| 153.42 | −423 | 1 | 246.01 | 1086 | 3 |
| 154.44 | −439 | 2 | 247.08 | 1199 | 2 |
| 155.40 | −444 | 1 | 249.04 | 1052 | 2 |
| 156.39 | −396 | 2 | 249.95 | 1088 | 3 |
| 157.43 | −478 | 1 | 251.00 | 884 | 2 |
| 158.43 | −452 | 2 | 254.25 | 1073 | 3 |
| 159.39 | −423 | 1 | | | |
| 160.60 | −452 | 1 | | | |

absolute values of $T^2 \ln \alpha$ calculated from the LVIFF least squares, coefficients are 3 percent larger than those calculated from the VPIE coefficients. On the other hand, over the common temperature range of the methyl fluoride VPIE data, 182–213 K, values of $T^2 \ln \alpha$ calculated from the LVIFF least squares, coefficients are 7 percent smaller than those calculated from the VPIE coefficients. Differences of comparable magnitude between LVIFF and reduced partition function ratios, $\ln (f_c/f_r)_{v_c, v_v}$, cf. (9) and (10), were found in previous measurements on both argon [4] and polyatomic fluids [26].

Table 2. Least squares fits of the LVIFF and VPIE data of the $CD_3H$–$CH_4$ and $CD_3F$–$CH_3F$ systems. Units: $A_1$: K$^2$, $B_1$: K, $A_2$: K$^2$ cm$^3$ g$^{-1}$, $B_2$: K cm$^3$ g$^{-1}$, $C_2$ cm$^3$ g$^{-1}$; $A_3$: K$^2$ cm$^6$ g$^{-2}$, $B_3$: K cm$^6$ g$^{-2}$.

| | Methane $T_0=100$ | Methyl fluoride $T_0=180$ |
|---|---|---|
| | $T^2 \ln \alpha = A_1 - B_1 (T-T_0) + C_1 (T-T_0)^2$ | |
| $A_1$ | −124.6 ±15.8[a] | 1333.5 ±28.8[a] |
| | −120.2 ± 1.0[b] | 1425.3 ± 4.7[c] |
| $B_1$ | +9.550 ± 1.141[a] | +4.194 ±0.621[a] |
| | +8.687 ± 0.06[b] | +4.444 ±0.046[c] |
| $C_1$ | +0.0711 ± 0.0171[a] | 0[a] |
| | 0[b] | 0[c] |
| | $T^2 \ln \alpha/(\varrho_l-\varrho_v) = A_2 - B_2 (T-T_0) + C_2 (T-T_0)^2$ | |
| $A_2$ | −299.7 ±42.0[a] | 1447.3 ±37[a] |
| $B_2$ | + 21.09 ± 3.03[a] | + 0.427 ±0.086[a] |
| $C_2$ | 0.0471 ± 0.0455[a] | 0 |
| | $T^2 \ln \alpha/(\varrho_l-\varrho_v)/(\varrho_c+\varrho_l+\varrho_v) = A_3 - B_3 T$ | |
| $A_3$ | 3103 ±280[a] | 1589 ±45[a] |
| | 3108[d] | |
| $B_3$ | 36.04 ±1.20[a] | −2.11 ±0.74[a] |
| | 35.44[e] | |

[a] This research.
[b] G. T. Armstrong, F. G. Brickwedde, and R. B. Scott [20].
[c] T. Oi, J. Shulman, A. M. Popowicz, and T. Ishida [21].
[d] Calculated for the temperature range 90–112 K from the ***F*** matrix in Table IX of [2].
[e] Calculated from the data in Table X of [22] and (A I.3).

Table 3. Absolute contributions (in K) of translation, rotation and internal vibration to $T \ln (f_c/f_r)$ as a function of temperature.

| Mode | $CD_3H$–$CH_4$ mixtures | | $CD_3F$–$CH_3F$ mixtures |
|---|---|---|---|
| | 111 K | 140 K[a] | 153 K[d] |
| Translation ($A/T$) | 1.97[b] | 1.56 | 1.58 |
| Rotation ($A/T$) | 5.24[b] | 4.16 | 2.42 |
| Internal vibrations ($B$) | 9.26[b] | 9.26 | −6.16[e] |
| $T \ln (f_c/f_r)$ | −2.05[b] | −3.65 | 10.16 |
| $T \ln (f_c/f_r)$ least squares | −1.95[c] | −3.34[c] | 10.10 |

[a] These values correspond to a linear extrapolation of $T^2 \ln \alpha$ vs. $T$(1).
[b] Calculated from Table X of [22].
[c] Calculated from a least squares fit of the data of Armstrong, Brickwedde and Scott, cf. Table V of [2].
[d] Calculated from Tables IV and VIII of [21].
[e] Calculated through (A I.3).

Singh and Van Hook [26] have shown that an isotope mixture is not ideal because of the difference in the molal volumes of the pure components. They have calculated the non-ideal behavior for a number of substances in good agreement with experiment. For the monatomic fluid, the non-ideal behavior leads to

a negative value of $\ln \gamma'$, the logarithm of the activity coefficient of the light isotope, when the concentration of the heavy isotope approaches zero. Thus the value of $\ln \alpha$ is smaller than $\ln (f_c/f_r)_{v_c, v_v}$ derived from vapor pressure measurements. This is the result found for $^{36}Ar$–$^{40}Ar$ mixtures. For the polyatomic molecule there are contributions to the molal volume isotope effect both from the intermolecular potential and the molecular vibrations. This can lead to both positive and negative values of $\ln \gamma'$. In a qualitative way, the Singh-Van Hook theory nicely explains the difference in signs between the deviations of the LVIFF and VPIE data for the $CD_3H$–$CH_4$ and $CD_3F$–$CH_3F$ systems. We will analyze the LVIFF data without making a correction for $\ln \gamma'$. This will not affect the analysis of the data.

## Discussion

From the triple point of methane, 90.7 K, to 120 K $T^2 \ln \alpha$ for the $CD_3H$–$CH_4$ mixture is a linear function of the temperature. This does not imply that $A$ and $B$ in (1) derived from a least squares fit of the experimental data are directly comparable with values calculated from molecular data through (2) and (3). Equation (1) is an approximate equation even in the harmonic oscillator approximation. For comparison of model calculations with experiment one can compare experimental values of $\ln \alpha$ with model values calculated as a function of temperature. One can also do a least squares fit of the values of $\ln \alpha$ from model calculations to an equation of the $A$–$B$ form and compare these with the $A$ and $B$ values derived from experiment. The latter method gives good agreement between experimental and calculated values for the liquid deuteromethanes over the temperature range 90.7–120 K [22]. The last squares values of $A$ and $B$ for the LVIFF $CD_3H$–$CH_4$ data in this temperature range are close to those calculated from (2) and (3), respectively. Above 120 K the linear approximation of $T^2 \ln \alpha$ as a function of $T$ no longer holds. At 160 K, the highest temperature of the present measurements, the experimental value is 35% smaller than that obtained from a linar extrapolation of the low temperature data. The $T^2 \ln \alpha$ vs. $T$ plot for the $CD_3H$–$CH_4$ mixture appears to have a minimum near 160 K, the highest temperature of the present measurements. $T^2 \ln \alpha$ must go to zero at the critical temperature. Within the precision of our data, there is no curvature in a $T^2 \ln \alpha$ vs. $T$ plot for the $CD_3F$–$CH_3F$ mixture over the temperature range 182–254 K.

From the molecular parameters derived from spectroscopic data and vapor pressure data in the temperature range 90.7–120 K [22] one finds the relative contributions of translation, rotation and internal vibration to the liquid-vapor isotope fractionation factor in the $CD_3H$–$CH_4$ system given in Table 3. The relative absolute magnitudes of the contributions of the internal vibrations, hindered rotation and translation to the logarithm of the LVIFF are 9:5:2 at 111 K. The internal vibrations dominate the LVIFFs even more at higher temperatures. The LVIFF data on argon [4] and carbon monoxide [15] show conclusively that $(\langle V^2 U\rangle_l - \langle V^2 U\rangle_v)$ and $(\langle O^2 U\rangle_l - \langle O^2 U\rangle_v)$ decrease with temperature and go to zero at the critical temperature. This behavior is also expected for $\sum_i [v'_{il} - v'_{iv}) - (v_{il} - v_{iv})]$ for the molecular vibrations. It must hold for each vibration.

We extend the method [13] used to obtain the temperature dependence of $(\langle V^2 U\rangle_l - \langle V^2 U\rangle_v)$ to develop the temperature dependence of $\langle v_{il}\rangle - \langle v_{iv}\rangle$. The method assumes that the intermolecular potential is pairwise additive and utilizes a power series expansion of the pair correlation function in the particle density up to terms in $\varrho^2$ [27]. From these assumptions one obtains

$$\langle v_{il}\rangle - \langle v_{iv}\rangle = \frac{\Delta v_{ic}}{(1+\gamma_i)\,\varrho_c^2}\,(\varrho_l - \varrho_v)\,[\varrho_c + \gamma_i(\varrho_l + \varrho_v)], \tag{18}$$

where $\Delta v_{ic} = (\langle v_{ic}\rangle - v_{ig})$ and $\gamma_i$ is the coefficient of $\varrho^2$ in the power series expansion. $v_{ig}$ is the frequency in the ideal gas. Lee and Bigeleisen [13] found the coefficient of $\varrho^2$ for the power series expansion of $\langle V^2 U\rangle$ to be close to one. $\langle O^2 U\rangle$ is a least quadratic in the density [15]. The approximation that the density dependence of $\langle V^2 U\rangle$, $\langle O^2 U\rangle$ and $\langle v_{il}\rangle - v_{ig}$ are each of the form $\varrho^*(1+\varrho^*)$ greatly simplifies the analysis of the LVIFF data. In fact, the data are not sufficiently extensive nor accurate to warrant the introduction of different coefficients for the quadratic terms in the density expansions of $\langle V^2 U\rangle$, $\langle O^2 U\rangle$ and $(\langle v_{il}\rangle - v_{ig})$. With this approximation (2) and (3) reduce to the form of (17). In Appendix A. I we show that when the coefficient 1/2 in (3) is replaced by $G(u_i) = (1/2 - 1/u_i + 1/(e^{u_i} - 1)$ the $B$ term in (1) includes the terms

$$\sum_i \ln (u_i/u'_i)_l/(u_i/u'_i)_v \quad \text{and}$$

$$\sum_i \ln [(1-e^{-u'_i})/(1-e^{-u_i})]_l/[(1-e^{-u'_i})/(1-e^{-u_i})]_v.$$

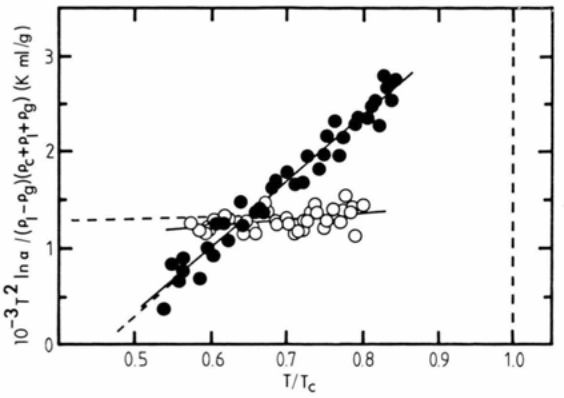


Fig. 4. Plots of the LVIFF data of $T^2 \ln\alpha/(\varrho_l-\varrho_v)/(\varrho_c+\varrho_l+\varrho_v)$ vs. $T/T_c$.
○, $+\ln\alpha\,(CD_3F/CH_3)_l/(CD_3H/CH_3F)_v$;
●, $-\ln\alpha\,(CD_3H/CH_4)_l/(CD_3H/CH_4)_v$; ----- least squares fits of VPIE data of [21] (methyl fluoride) and [20] (methane).

In Figs. (2) and (3) are plotted $T^2 \ln\alpha/(\varrho_l-\varrho_v)$ vs. $T$ for the $CD_3H$–$CH_4$ and $CD_3F$–$CH_3F$ systems, respectively. The first term in the power series expansion of the density, $(\varrho_i-\varrho_v)$, accounts for almost all the curvature in the $T^2 \ln\alpha$ vs. $T$ plots. In fact, for the mixture $CD_3F$–$CH_3F$ the slope $B_2$ is near zero. Finally, plots of $T^2 \ln\alpha/(\varrho_l-\varrho_v)(\varrho_c+\varrho_l+\varrho_v)$ vs. $T^*=T/T_c$, Fig. 4, are strictly linear over the temperature ranges of the LVIFF and VPIE data.

Least squares fits appropriate to (15)–(17) are given in Table 2, where we also give values of $A_3$ and $B_3$ calculated from the cell model (Table V of [22]) for the $CD_3H$–$CH_4$ system. The agreement is within the limits of the precision of the LVIFF experiments. This supports our interpretation of the temperature coefficient of the LVIFF data for the $CD_3H$–$CH_4$ system and adds credibility to the cell model calculations for the deuteromethanes [22].

An analysis of the temperature coefficients of the VPIE and LVIFF data for the $CD_3F$–$CH_3F$ system suggests a reinterpretation given the VPIE data [21]. A least squares fit of the VPIE data to (15) with $C_1=0$ gives $B_1=4.444\pm0.046$ K. Attempts to reproduce the VPIE data using the cell model with a temperature dependent $\boldsymbol{F}$ matrix give $B_1=-6.16$ K, cf. Table 3. Clearly, the least squares, constants, $A_1$ and $B_1$, for $CD_3F$–$CH_3F$ have little meaning within the framework of the cell model calculations. The LVIFF data lead to a value of $B_2=0.427\pm0.086$ K cm$^3$ gm$^{-1}$. Over the temperature range of the VPIE data, 132–213 K, $\Delta\varrho$ varies from 1.00 to 0.84 gm cm$^{-3}$. At 190 K the value of $B_1$ calculated from $B_2$ is 0.38 K, one order of magnitude smaller than the least squares value of $B_1$ and opposite in sign to that calculated with the temperature dependent $\boldsymbol{F}$ matrix [21]. Most of the least squares value of $B_1$ arises from the temperature dependence of $A_1$, the translation and rotation in liquid methyl fluoride. We can compare the LVIFF values of $A_3$ and $B_3$ of (17) with values calculated for the temperature 153 K from the cell model using the calculations given in Tables IV and VIII of [21], $A_{\boldsymbol{F}\,\text{matrix}}$ and $B_{\boldsymbol{F}\,\text{matrix}}$, after correction of the latter for the factor $\Delta\varrho\,(\varrho_c+\varrho_l+\varrho_v)$.

| | $A$ | | $B$ |
|---|---|---|---|
| $A_{\boldsymbol{F}\,\text{matrix}}$ | 519 K$^2$ cm$^6$ gm$^{-2}$ | $B_{\boldsymbol{F}\,\text{matrix}}$ | $-5.22$ K cm$^6$ gm$^{-2}$ |
| $A_3$ | $1589\pm45$ | $B_3$ | $-2.11\pm0.74$ |

This suggests a revision of the $\boldsymbol{F}$ matrix used in the cell model calculations [21] along the following lines. The sum of the isotope shifts from the gas to the liquid should be reduced by a factor of three. The diagonal $\boldsymbol{F}$ matrix elements of Table VII in [21] should be increased by about a factor of three and a temperature dependence in accord with (17) should be introduced for the translation and rotation force constants.

## Conclusion

Measurements of the temperature dependence of the LVIFF for a dilute solution of $CD_3H$ in $CH_4$, when combined with the VPIE data for the pure substances, show that $T^2 \ln\alpha$ is proportional to the density difference, $(\varrho_l-\varrho_v)$ times the sum of the liquid and vapor densities, over the temperature range 91–160 K. The zero point energy difference between the internal vibrations in the real gas and the liquid is proportional to $(\varrho_l-\varrho_v)(\varrho_c+\varrho_l+\varrho_v)$. This density dependence has been found previously for $\langle V^2U\rangle_l-\langle V^2U\rangle_v$ and is consistent with data for $\langle O^2U\rangle_l-\langle O^2U\rangle_v$. The separation factor goes to unity at the critical temperature through the term $(\varrho_l-\varrho_v)$, which has been established for each mode that contributes to the condensed phase isotope effect. Good agreement is found for $T^2 \ln\alpha/(\varrho_l-\varrho_v)(\varrho_c+\varrho_l+\varrho_v)$ with previous cell model calculations for the deuteromethanes. A similar analysis of the VPIE and LVIFF data of the $CD_3F$–$CH_3F$ indicates directions for the revision of the cell model calculations for methyl fluoride.

The present LVIFF measurements bring to a conclusion thirty five years of theoretical and experimen-

tal work on condensed phase isotope effects. During this time the precision of the experimental data has been improved by an order of magnitude. The development of the statistical mechanical theory of condensed phase isotope effects and its application to selected systems have uncovered a wealth of material relevant to the mean squares force, the mean square torque and the perturbations of the molecular vibrations by the intermolecular force field in liquids and solids. In the case of monatomic fluids quantitative agreement has been found between condensed phase isotope effect measurements and molecular dynamics and perturbation theory calculation. We have yet to attain the necessary degree of refinement in the calculation of intermolecular forces and molecular dynamics for the calculation of condensed phase isotope effects of polyatomc fluids. We can set as a goal for Dr. Karl Heinzinger's 70. Geburtstag sufficient progress in a priori calculations for molecular systems such that one will be able to make calculations relevant to all the fine details that can be studied through condensed phase isotope effects.

## Appendix I

In this Appendix we derive a convenient correction to (1) within the assumption that the molecular vibrations in the condensed and vapor phases are harmonic oscillators. Comparison of (3.5) of [2], with (3) leads to the following correction to (1):

$$\mathrm{Corr}\,(1)=\sum_i^{\mathrm{int}}\{\ln\,(u_i/u_i')_c/(u_i/u_i')_v + \ln\,[(1-e^{-u_i})/(1-e^{-u_i})]_c/[(1-e^{-u_i'})/(1-e^{-u_i})]_v\}. \tag{A I.1}$$

We now follow the procedure of [2] and expand $u_{iv}'$ around $u_{ic}'$ and $u_{iv}$ around $u_{ic}$. The expansion leads to

$$\mathrm{Corr}\,(1)=\sum_i[(\exp\,(u_i')-1)^{-1}-1/u_i']_v\,(u_{ic}'-u_{iv}')] - \sum_i[(\exp\,(u_i)-1)^{-1}-1/u_i]_v\,(u_{ic}-u_{iv})]. \tag{A I.2}$$

When (A I.2) is added to (3), and one takes note of the fact that $B$ is defined with respect to $(v_v'-v_c')-(v_v-v_c)$, one obtains

$$B\,(\mathrm{corr})=\sum_i G\,(u_i')_v\,(v_v'-v_c')-G\,(u_i)_v\,(v_v-v_c), \tag{A I.3}$$

where $G\,(u_i)=[1/2+(\exp\,(u_i)-1)^{-1}-1/u_i]$. $B\,(\mathrm{corr})$ is not a temperature independent term even in the harmonic oscillator approximation. Its temperature coefficient is small. Replacement of the zero point energy coefficient, 1/2, in the usual $B$ equation by $G\,(u)$ leads to corrections of 5 and 15 percent for C–H stretching and $CH_2$ bending vibrations, respectively, at 100 K. This correction in the form of $\sum_i^{\mathrm{int}}\ln\,(u_i/u_i')_1/(u_i/u_i')_v$ has been discussed previously by Stern, Van Hook, and Wolfsberg [28].


[1] G. Jansco and W. A. Van Hook, Chem. Rev. **74,** 689 (1974).
[2] J. Bigeleisen, J. Chem. Phys. **34,** 1485 (1961).
[3] I. Oppenheim and A. S. Friedman, J. Chem. Phys. **35,** 35 (1961).
[4] J. T. Phillips, C. U. Linderstrom-Lang, and J. Bigeleisen, J. Chem. Phys. **56,** 5053 (1972).
[5] Z. Bilkadi, M. W. Lee and J. Bigeleisen, J. Chem. Phys. **62,** 2087 (1975).
[6] J. Bigeleisen and E. Roth, J. Chem. Phys. **35,** 68 (1961).
[7] J. Bigeleisen, F. P. Brooks, T. Ishida, and S. V. Ribnikar, Rev. Sci. Instrum. **39,** 353 (1968).
[8] F. J. Torre, D. M. Eshelman, M. W. Lee, P. Neufeld, and W. Watson, Rev. Sci. Instrum. **47,** 1142 (1976).
[9] W. A. Van Hook, J. Chem. Phys. **44,** 234 (1966).
[10] T. Ishida and J. Bigeleisen, J. Chem. Phys. **49,** 5498 (1968).
[11] J. Bigeleisen, S. Fuks, S. V. Ribnikar, and Y. Yato, J. Chem. Phys. **66,** 1689 (1977).
[12] J. Bigeleisen, S. V. Ribnikar, and W. A. Van Hook, J. Chem. Phys. **38,** 497 (1963).
[13] M. W. Lee and J. Bigeleisen, J. Chem. Phys. **67,** 5634 (1977).
[14] We retain the isotope separation factor scaling exponent, b, of [4] and modify the nomenclature of [13] appropriately.
[15] D. Götz, M. W. Lee and J. Bigeleisen, J. Chem. Phys. **70,** 5731 (1979).
[16] G. Jansco and W. A. Van Hook, Can. J. Chem. **55,** 3371 (1977); Chem. Phys. Lett. **48,** 481 (1978).
[17] J. Warner and M. Wolfsberg, J. Chem. Phys. **78,** 1722 (1983).
[18] B. Maessen and M. Wolfsberg, Z. Naturforsch. **38a,** 191 (1983).
[19] M. Wolfsberg, J. Chem. Phys. **80,** 3087 (1984).
[20] G. T. Armstrong, F. G. Brickwedde, and R. B. Scott, J. Res. Nat'l. Bur. Standards, **55,** 39 (1955).
[21] T. Oi, J. Shulman, A. Popowicz, and T. Ishida, J. Phys. Chem. **87,** 3153 (1983).
[22] J. Bigeleisen, C. B. Cragg, and M. Jeevanandam, J. Chem. Phys. **47,** 4335 (1967).
[23] D. M. Eshelman, F. J. Torre, and J. Bigeleisen, J. Chem. Phys. **60,** 420 (1974).
[24] J. Bigeleisen, M. L. Perlman, and H. C. Prosser, Anal. Chem. **24,** 1356 (1952).
[25] I. Friedman, Geochim. Cosmochim. Acta **4,** 89 (1953).
[26] R. R. Singh and W. A. Van Hook, J. Chem. Phys. **86,** 2969 (1987).
[27] C. G. Gray and K. E. Gubbins, Theory of Molecular Fluids, Vol. I. Clarendon Press, Oxford 1984, pp. 164, 206.
[28] M. J. Stern, W. A. Van Hook, and M. Wolfsberg, J. Chem. Phys. **39,** 3179 (1963).